Supplementary Materials for"Site-Controlled Ge Hut Wire-Based Multiple Quantum Dots with Integrated Charge Sensing Capability"

Jin Leng,[1,2,3] Fei Gao,[4,5] Yu-Chen Zhou,[1,2,3] Chu Wang,[1,2,3] Hao-Tian Jiang,[1,2,3] Zhi-Tao Wu,[1,2,3] Gang Cao,[1,2,3,6] Jianjun Zhang,[4,6] Hai-Ou Li,[1,2,3,6*] and Guo-Ping Guo[1,2,3,6]

[1] *Laboratory of Quantum Information, University of Science and Technology of China, Hefei, Anhui 230026, China*

[2] *Anhui Province Key Laboratory of Quantum Network, University of Science and Technology of China, Anhui 230026, China*

[3] *CAS Center for Excellence and Synergetic Innovation Center in Quantum Information and Quantum Physics, University of Science and Technology of China, Hefei, Anhui 230026, China*

[4] *Institute of Physics, Chinese Academy of Sciences, Beijing 100190, China*

[5] *Qilu Institute of Technology, Jinan, 250200, China*

[6] *Hefei National Laboratory, Hefei 230088, China*

[*]Corresponding author: haiouli@ustc.edu.cn;

S1. Charge-sensing measurement circuit and principle

Fig.S1 shows the schematic of the wiring used for our charge-sensor measurements. The measurement method we used is called modulation measurement. We apply a DC bias V_{bias} to the drain of the CS-QD (the lower-left QD in the device) using an isolated voltage source in combination with a voltage divider. The source of the CS-QD is connected to the lock-in amplifier measurement input. The lock-in's excitation output is routed through a summer to the measured QD's gate g3, so that a small AC excitation $V_{ac}cos(\omega t)$ is superimposed on the gate bias U_{g3}. The lock-in amplifier selectively detects and amplifies signals at the reference frequency ω.

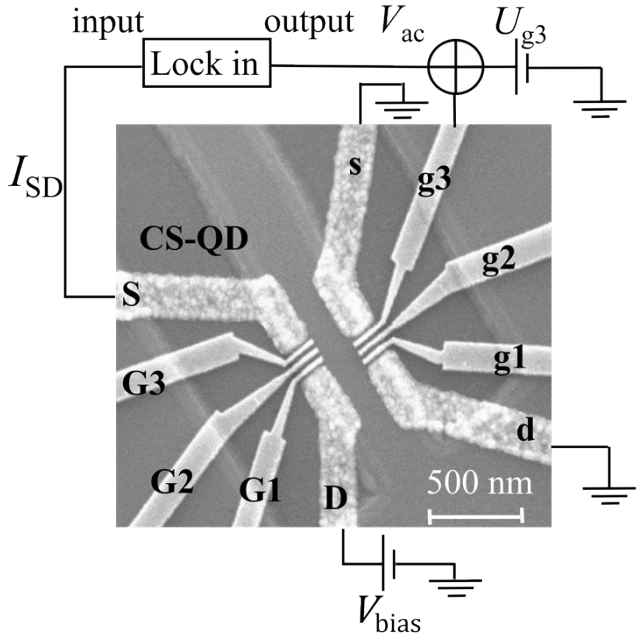

Fig.S1 Schematic diagram of charge sensor measurement circuit.

In the measurement the CS-QD is tuned to a Coulomb peak. When the charge on the measured QD changes, capacitive coupling shifts the CS-QD Coulomb peak and produces a step in the transport current I_{SD}. Thus, the charge change in the measured QD can be detected by the differential response of I_{SD} with respect to the measured QD gate. In our case we measure the differential signal dI_{SD}/dU_{g3}.

Formally, I_{SD} can be written as a function of the instantaneous gate voltage: $I_{SD}(U_{g3} + V_{ac}cos(\omega t))$.

Taylor expanding to first order gives

$$I_{SD}\left(U_{g3} + V_{ac}\cos(\omega t)\right) \approx I_{SD}\left(U_{g3}\right) + \frac{dI_{SD}}{dU_{g3}} * V_{ac}cos(\omega t) \quad \text{(S1)}$$

The AC current component at frequency ω therefore has amplitude

$$I_{\omega} = \frac{dI_{SD}}{dU_{g3}} * V_{ac} \quad \text{(S2)}$$

The lock-in detects this AC component at ω, from the measured signal the differential conductance dI_{SD}/dU_{g3} can be obtained, and thereby enables charge-sensing measurement of QD.

S2. Simulation model of the triple quantum dot phase diagram

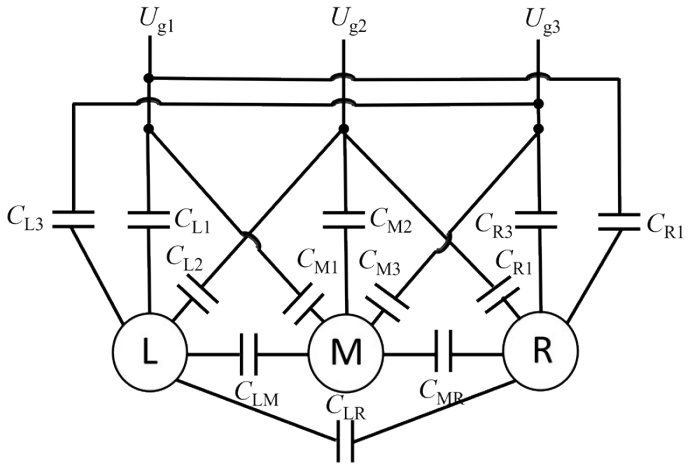

Fig.S2 Schematic diagram of the equivalent capacitance model of the TQD System.

Our TQD simulations are based on the classical model used in Ref. 44. Fig.S2 shows the equivalent capacitance model of the TQD system. The charges on the dots and gates can be expressed in matrix form as

$$\begin{bmatrix} Q_D \\ Q_g \end{bmatrix} = \begin{bmatrix} C_{DD} & C_{Dg} \\ {C_{Dg}}^T & C_{gg} \end{bmatrix} \begin{bmatrix} U_D \\ U_g \end{bmatrix} \tag{S3}$$

Where $Q_D = [Q_L, Q_M, Q_R]^T$, $Q_g = [Q_{g1}, Q_{g2}, Q_{g3}]^T$ are the charge vectors on the QDs and gates, respectively. The QD charges satisfy $Q_D = eN_D$, $N_D = [N_L, N_M, N_R]^T$ being the electron number vector on each QD. $U_D = [U_L, U_M, U_R]^T$, $U_g = [U_{g1}, U_{g2}, U_{g3}]^T$ are the voltage vectors of the QDs and gates. C_{DD}, C_{Dg}, and C_{gg} denote the capacitance matrices between QDs, between QDs and gates, and between gates, respectively. Since the electrostatic potential of the gates is determined by externally applied voltages and is independent of the gate–gate capacitance, C_{gg} only affects the energy zero point and can therefore be set to zero.

The free energy of the system is given by

$$F = U - V = \frac{1}{2}\begin{bmatrix} {Q_D}^T & {Q_g}^T \end{bmatrix} \begin{bmatrix} U_D \\ U_g \end{bmatrix} - {U_g}^T Q_g$$

$$= \frac{1}{2e^2} {Q_L}^{eff} \left(E_L {Q_L}^{eff} + E_{LM} {Q_M}^{eff} + E_{LR} {Q_R}^{eff} \right) + \frac{1}{2e^2} {Q_M}^{eff} \left(E_{LM} {Q_L}^{eff} + E_M {Q_M}^{eff} + E_{MR} {Q_R}^{e}$$
$$\frac{1}{2e^2} {Q_R}^{eff} \left(E_{LR} {Q_L}^{eff} + E_{MR} {Q_M}^{eff} + E_R {Q_R}^{eff} \right)$$

(S4)

Where,

$${Q_X}^{eff} = eN_X + C_{Xg1}U_{g1} + C_{Xg2}U_{g2} + C_{Xg3}U_{g3}$$
$$E_X = K\left(C_Y C_Z - {C_{YZ}}^2\right)$$
$$E_{XY} = K\left(C_Z C_{XY} + C_{XZ} C_{YZ}\right)$$
$$K = e^2/\left(C_L C_M C_R - 2C_{LM} C_{LR} C_{MR} - C_R C_{LM} - C_M C_{LR} - C_L C_{MR}\right)$$

X,Y,Z represent cyclic permutations of the QDs L,M,R. ${E_L}$, ${E_M}$, and ${E_R}$are the charging energies of the three QDs, while ${E_{LM}}$, ${E_{MR}}$, and ${E_{LR}}$are the electrostatic coupling energies between the QDs. These parameters can be extracted by fitting the charge stability diagrams and the anticrossings of the energy levels. The QD–gate capacitance matrix ${C_{Dg}}$can be approximately obtained from the charge stability diagram by the gate voltage change required to add one electron to a QD, i.e., ${C_{Dg}} = e/\Delta U_g$. After extracting the parameters related to the left and right QDs from the phase diagram, the parameters associated with the middle QD can be obtained by converting the ratios of charge addition line shifts under different ${U_{g2}}$. This procedure yields Eqs. (2)–(4) in the main text.

Once these parameters are determined, the free energy ${F}$depends only on the charge configuration $(N_L,N_M,N_R)$and the gate voltages ${U_{g1}},{U_{g2}},{U_{g3}}$. By numerically minimizing the free energy ${F}$, the ground-state stability diagram of the TQD system can be obtained.